Some of his results have been presented in our previous paper.[1a] The vapor spectra resemble those from the matrix sample, but the bands are much broader and more strongly overlapped. The similar spectral patterns observed for the matrix and for the vapor spectra of the thiouracils studied, particularly for the S-methylated thiouracils, suggest that the tautomeric forms present in the vapor phase are the same as those present in the matrix.

Conclusions

The main conclusions from this study are as follows.

(1) 2-Thiouracil, and 4-thiouracil and their N1- or N3-methylated derivatives as well as 2,4-dithiouracil all exist predominantly in the oxothione or dithione tautomeric form in an inert matrix environment (and also in the vapor phase).

(2) In contrast, S2- and S4-methylated derivatives of thiouracils adopt both hydroxy and oxo tautomeric forms under the same matrix (and vapor) conditions. For S2-methylated uracil the oxo tautomer predominates, while for 4-(methylthio)-6-methyluracil the hydroxy form dominates.

(3) Substitution of sulfur for oxygen results in a drastic change of almost the entire spectrum in addition to the obvious changes in the C=O and C=S stretching and bending regions. Strong intensity changes are also found for the C=C stretching, the NH bending (?) modes near 1640 and 1550 cm^{-1} respectively.

(4) The effect of sulfur substitution on N1H and N3H frequencies and intensities reflects changes in proton donor abilities of these groups. This is expected to affect the strength of hydrogen bonding in which they participate, particularly that formed by the biologically significant N3H group. This effect should be taken into account in addition to the generally recognized influence on the hydrogen bonding (and on stacking or surface interactions) resulting from the change of the proton accepting group from C4=O or C2=O to C4=S or C2=S.

(5) Our study suggests that C2=S and C4=S stretching modes appear as relatively strong bands in the region near 1070-1150 cm^{-1}, but they are much more strongly coupled with the vibrations of other groups then in the case of the C=O stretches.

(6) Calculations at the SCF(3-21G*) level appear to be useful for interpretation of the general features of the IR matrix spectra of isolated molecules, but they are not good enough to account for the out-of-plane modes.

(7) Finally, calculations at the SCF(3-21G*) + MBPT(2) [or even at the SCF(6-31G**) + MBPT(2) level] level performed for model compounds in which the methyl group was replaced by a hydrogen atom do not predict correctly the tautomeric equilibria for both the S2- and S4-methylated thiouracils. Hence, experimental infrared matrix studies still provide a necessary test of the reliability of the calculations of tautomeric equilibria.

Note Added in Proof. A recent ab initio calculation (HF, MBPT, CC) by Les and Adamowicz[53] for S2 and S4 methylated thiouracils is in much better agreement with our experimental data.

Acknowledgment. We thank Professor D. Shugar (Warsaw) for his suggestion to undertake studies of thiouracils, for valuable discussions, and for supplying us with these compounds from his collection. We are also grateful to Dr. A. Barski for providing us with his unpublished results for the gas phase. This work was supported by the Ministry of National Education Project CPBP 01.12 (in Warsaw) and by NIH Research Grant No. 32988 (in Gainesville). J.L. thanks the Alabama Supercomputer Network for allotment of computer time for the calculations presented here.

Supplementary Material Available: Tables of symmetry coordinates of the thiouracil tautomers and description of vibrational modes (Table 7), force constants of 2-thiouracil, 4-thiouracil, and 2,4-dithiouracil (calculated by the ab initio 3-21G* method) (Tables 8-10), and frequencies, intensities, and potential energy distributions of 2-mercaptouracil and 4-mercaptouracil (calculated by the ab initio 3-21G* method) (14 pages). Ordering information is given on any current masthead page.

A Theoretical Investigation of the Thermal Ring Opening of Cyclopropyl Radical into Allyl Radical. Evidence for a Highly Nonsymmetric Transition State

Santiago Olivella,*,† Albert Solé, and Josep M. Bofill

Contribution from the Departaments de Química Orgánica and Química Física, Universitat de Barcelona, Martí i Franquès 1, 08028-Barcelona, Catalunya, Spain. *Received August 3, 1989*

Abstract: An ab initio investigation of the thermal ring opening of cyclopropyl radical (**1**) to give allyl radical (**2**), with geometries optimized at the UHF/3-21G and CASSCF/3-21G levels of theory, predicts a highly nonsymmetric structure for the transition state of such an electrocyclic reaction. Thus, the CASSCF/3-21G-optimized transition structure corresponds to rotation of one of the methylene groups in **1** through 24° while the other remains orthogonal to the plane of the carbon atoms, the length of the CC bond undergoing rupture being 2.066 Å. The present results agree with those of early MINDO/3 calculations by Dewar and Kirschner in the important respect that the minimum-energy reaction path does not involve synchronous rotation of the methylene groups, so that one methylene rotation is almost completed before the other commences. As a consequence, both conrotatory and disrotatory ring-opening modes of **1** involve a common transition state.

The thermolysis of cyclopropyl radical (**1**) leading to ring opening and allyl radical (**2**) formation or, conversely, the cyclization of **2** into **1** is the simplest example of an electrocyclic reaction of a free radical. During the reaction the methylene groups may move in either a disrotatory or conrotatory fashion. Unlike the case of the cyclopropyl cation and anion, no conclusion may be drawn from the Woodward-Hoffmann rules,[1] from the orbital and state correlation diagrams,[2] or from PMO arguments[3]

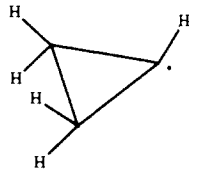

1

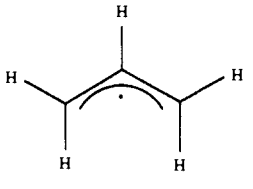

2

† On leave of absence from the C.S.I.C.

(1) Woodward, R. B.; Hoffmann, R. *Angew. Chem., Int. Ed. Engl.* **1969**, *8*, 781.

(2) Longuet-Higgins, H. C.; Abrahamson, E. W. *J. Am. Chem. Soc.* **1965**, *87*, 2045.

(3) See: Dewar, M. J. S. *The Molecular Orbital Theory of Organic Chemistry*; McGraw-Hill: New York, 1968; pp 325-339.

0002-7863/90/1512-2160$02.50/0

about the mode of reaction of **1**. Moreover, no experimental evidence is available. Several theoretical studies, both semiempirical[4-9] and ab initio,[10,11] have therefore been devoted to establishing the preferred ring-opening mode of **1**. Early extended-Hückel calculations[4] predicted conrotatory ring opening, but semiempirical calculations based on the MINDO/2 method indicated a disrotatory mode.[5,6,8] Subsequently, Dewar and Kirschner[7] reinvestigated the problem using the MINDO/3 method and found only one transition state interconverting **1** and **2**, its structure corresponding to rotation of one of the methylene groups in **1** through 50° while the other remains orthogonal to the plane of the carbon atoms, so that both disrotatory and conrotatory reactions involve a common transition state. Although this result was quite novel, it appears that has been overlooked.

To our knowledge, only two ab initio studies have been reported previously on the electrocyclic interconversion between **1** and **2**. The first one was carried out by Farnell and Richards 16 years ago.[10] In that study the potential energy curves of both conrotatory and disrotatory pathways were calculated with a minimum basis set, by linear interpolation assuming synchronous rotation of both methylene groups and keeping the methine hydrogen in the plane of the carbon atoms. It was concluded that the ring opening of **1** is formally forbidden in both modes, but that if distortion of the molecule occurs a near-disrotatory reaction would be preferred. Shortly after, Peyerimhoff et al.[11] reported approximately calculated ab initio potential energy curves for the electrocyclic isomerization of **1** to **2**, obtained via Koopmans' theorem from the self-consistent-field (SCF) energies, calculated with a double-ζ basis set for the corresponding (cyclopropyl/allyl) cation system. Those calculations suffered from several drawbacks: not all the geometrical parameters were varied simultaneously along the reaction paths, leading to an implicit arbitrary choice of reaction coordinate; the "transition regions" were located by means of a pointwise procedure, without use of any rigorous criterion for the characterization of a transition state. For these reasons, the conclusions drawn from that study, concerning the "stepwise" mechanism for both conrotatory and disrotatory reactions, where the rotation of the methylene groups would take place abruptly after the bond stretching, and the clear preference of the disrotatory reaction over the conrotatory one, have to be taken very cautiously.

As a part of a comprehensive theoretical study of the thermal rearrangement reactions in cycloalkyl and bicycloalkyl radicals, we report here the first ab initio molecular orbital investigation of the $C_3H_5^{\bullet}$ potential energy surface for the ring opening of **1** into **2**, using single-determinant and multiconfiguration wave functions, along with analytic energy gradient methods and force constant matrix analysis of the stationary points.

Elementary Theoretical Considerations

The first step in the present investigation was to determine the geometrical requirements for the transition states of the conrotatory and disrotatory isomerizations of **1** to **2**, as well as the characteristics of the electronic wave function describing these transition states. For this purpose, we carried out a detailed analysis of the orbital and state correlation diagrams of both pathways.

Figure 1 shows the correlation diagram for the molecular orbitals (MOs) most directly involved in the disrotatory interconversion between **1** and **2**. For **1**, they are the orbitals associated with the CC bond that is broken (σ_{CC} and σ_{CC}^*) and the single-occupied MO (SOMO) ($\sigma_C^{\bullet}$), while for **2**, they are the set of three π orbitals (π_1, π_2, and π_3). Each of these orbitals is classified by symmetry labels (S, symmetrical; A, antisymmetrical) relating to the symmetry plane that is maintained during the conventional disrotatory process, namely, the plane bisecting the central CC bond in **1**. Alternative symmetry labels appropriate to the irreducible representations (a′ or a″) of the C_s point group are also included. Assuming that the equilibrium geometry of **1** has C_s molecular symmetry,[12] its ground-state electron configuration can be written in short form as

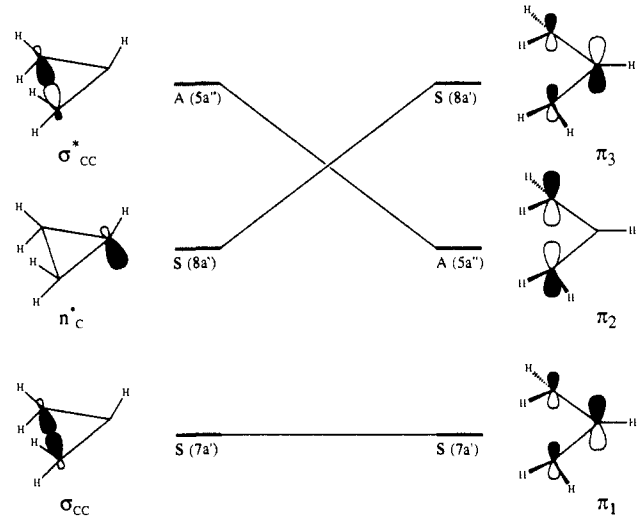

Figure 1. Molecular orbital correlation diagram for the disrotatory interconversion between cyclopropyl and allyl radicals.

$$...(6a')^2(3a'')^2(4a'')^2(7a')^2(8a')^1 \quad (1)$$

The equilibrium geometry of **2** has C_{2v} symmetry and its ground-state electron configuration is

$$...(3b_2)^2(4b_2)^2(6a_1)^2(1b_1)^2(1a_2)^1 \quad (2)$$

If C_{2v} molecular geometry is retained but the individual MOs are classified according to the lower symmetry point group C_s, then the ground-state electron configuration of **2** is written

$$...(3a'')^2(4a'')^2(6a')^2(7a')^2(5a'')^1 \quad (3)$$

From configurations 1 and 3 it follows that the ground states of **1** ($^2A'$) and **2** ($^2A''$) belong to different symmetry classes of the common point group C_s, and in order to conserve the orbital symmetry, the disrotatory thermal reaction would thus always have to give an electronically excited state of the product.

Consider now the alternative conrotatory pathway. Due to the fact that the methine hydrogen in **1** is bent out of the plane of the carbon atoms,[13] during the conventional conrotatory interconversion of **1** and **2** the molecular symmetry is destroyed and there is, strictly speaking, no symmetry in the transition state. Thus, all MOs are trivially symmetric and one cannot draw any significant orbital correlation diagram. Nevertheless, assuming C_{2v} symmetry for **1** (i.e., imposing planarity at the radical site), then in the conrotatory mode the system preserves a 2-fold axis of symmetry throughout the reaction, so that each MO may be classified according to the irreducible representations (a or b) of the C_2 point group as it is symmetric or antisymmetric about that axis. The situation is illustrated in Figure 2. In C_2 symmetry, the ground-state electron configuration for **1** is written in short form as

$$...(5a)^2(6a)^2(4b)^2(7a)^2(5b)^1 \quad (4)$$

whereas the ground-state electron configuration of **2** is written

$$...(3b)^2(4b)^2(6a)^2(5b)^2(7a)^1 \quad (5)$$

(4) Woodward, R. B.; Hoffmann, R. *J. Am. Chem. Soc.* **1965**, *87*, 395.
(5) Dewar, M. J. S.; Kirschner, S. J. *Am. Chem. Soc.* **1971**, *93*, 4290.
(6) Szeimies, G.; Boche, G. *Angew. Chem., Int. Ed. Engl.* **1971**, *10*, 912.
(7) Dewar, M. J. S.; Kirschner, S. *J. Am. Chem. Soc.* **1974**, *96*, 5244. Dewar, M. J. S. *Chem. Br.* **1975**, *11*, 97.
(8) Beran, S.; Zahradnik, R. *Collect. Czech. Chem. Commun.* **1976**, *41*, 2303.
(9) Bews, J. R.; Glidwell, C.; Walton, J. C. *J. Chem. Soc., Perkin Trans. 2* **1982**, 1447.
(10) Farnell, L.; Richards, W. G. *J. Chem. Soc., Chem. Commun.* **1973**, 334.
(11) Merlet, P.; Peyerimhoff, S. D.; Buenker, R. J.; Shih, S. *J. Am. Chem. Soc.* **1974**, *96*, 959.
(12) Depuis, M.; Pacansky, J. *J. Chem. Phys.* **1982**, *76*, 2511.
(13) Kochi, J. K.; Bakuszis, P.; Krusic, P. J. *J. Am. Chem. Soc.* **1973**, 1516.

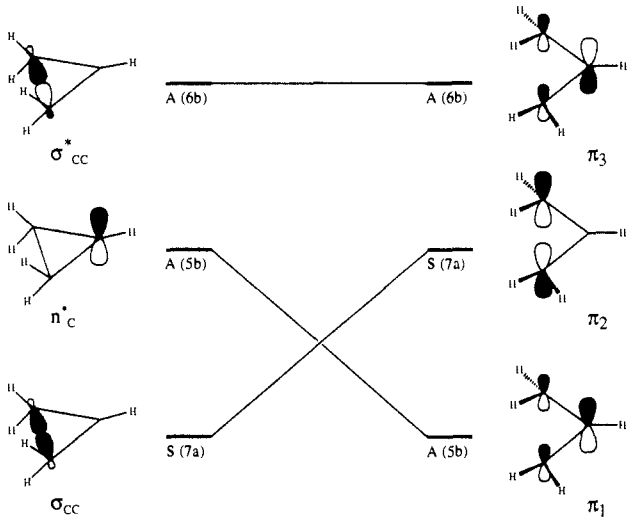

Figure 2. Molecular orbital correlation diagram for the conrotatory interconversion between cyclopropyl and allyl radicals.

Therefore, it turns out that the ground states of **1** (^{2}A) and **2** (^{2}B) again belong to different symmetry classes of the common point grou C_2, and in order to conserve the orbital symmetry, the conrotatory thermal reaction would thus have to give an electronically excited state of the product.

On the basis of the above orbital correlation analysis, it becomes apparent that the thermal interconversion between **1** and **2** is both orbital-symmetry forbidden and state-symmetry forbidden whichever mode, conrotatory, or disrotatory, is considered. It should be noted that, at variance with the symmetry-forbidden electrocyclic transformations of closed-shell systems, the electron interaction will not prevent the resulting crossing between the electron configurations 1 and 3 (disrotatory transformation) or 4 and 5 (conrotatory transformation) due to the fact that these pairs of configurations belong to different symmetry classes and do not interact. Therefore, it appears that *a configuration interaction (CI) treatment cannot force a correlation between the ground states of radicals 1 and 2*. This clearly suggests that the thermal electrocyclic rearrangement of **1** to **2** is a nonadiabatic reaction. However, this prediction seems to be in direct contradiction with the fact that the activation energy for the thermolysis of **1** leading to **2** in the gas phase is 22 ± 2 kal/mol.[14-17] For this reason, it seems unlikely that the reaction gives an electronically excited state of the product.

As pointed out first by Boche and Szeimies,[18] perturbation by *not fully concerted changes* in the geometrical parameters during the reaction can lead to a complete annulment of the symmetry of **1**, and consequently, this would allow an interaction between the aforementioned configurations of the unperturbed system, which in turn obviates the need for crossing (noncrossing rule) and forces the correlation between the ground states. On the basis of this suggestion, it appears that in order to locate a true transition structure on the potential energy surface for the interconversion between **1** and **2**, it is necessary to destroy the initial molecular symmetry along the reaction path, by performing adequate distorsions of the geometrical parameters in the sense of not allowing a synchronous change of their values from the reactant to the product.

At this point, it should be emphasized that the current geometry optimization routines based on variable metric minimization methods (e.g., either the Schlegel[19] or Murtagh–Sargent[20] multiparameter search routines) are molecular symmetry conservative. That is, these quadratic convergent methods generate improved points q^{n+1} from old points q^n by the recursion formula

$$q^{n+1} = q^n - \alpha_n \mathbf{A}^n g^n \qquad (6)$$

where g^n is the gradient of the potential energy function and the method of determining the scalar α_n and the matrix $\mathbf{A}^n$ depends on the variable metric method used. As shown in ref 21, each point q^{n+1} generated by eq 6 transforms according to the totally symmetric representation of the point group of q^n. It follows that if the transition-state search is carried out by employing the usual reaction coordinate method starting at the equilibrium geometry of the reactant, the symmetry of this molecule is approximately maintained along the calculated minimum-energy reaction path, so it is unlikely that with this procedure any transition state showing the required nonsymmetric structure can be located.

Concerning the requirements that the wave function has to fulfill, in order to describe adequately the essential electronic effects involved in either the electrocyclic disrotatory or conrotatory interconversion between **1** and **2**, we note that along each pathway the wave function should *at least* include the configurational interaction between the crossing pairs of configurations (i.e., 1 and 3 for disrotation or 4 and 5 for conrotation) by destroying the symmetry elements common to reactant and product. An obvious choice would be a multiconfigurational SCF wave function of the "complete active space" class. However, as in the case of the symmetry-forbidden pericyclic reactions of closed-shell systems, the single-determinant spin-unrestricted Hartree–Fock method may provide at much lower computational cost a description of the potential energy surface, which is qualitatively correct in the sense that the stationary points located by using this simple wave function may be close in geometry to those calculated by employing a CI approach.[22,23] As it will be shown later, this proves to be the case.

The Unrestricted Hartree–Fock Approximation as a Starting Point

Computational Details. The calculations reported in this section, denoted UHF/3-21G, were carried out within the framework of ab initio single-determinant spin-unrestricted Hartree–Fock (UHF) method[24] with the small 3-21G split-valence basis set,[25] employing a locally modified version[26] of the GAUSSIAN 80 system of programs.[27] The equilibrium geometries of **1** and **2** were fully optimized subject to specified symmetry constraints (C_s and C_{2v} point groups, respectively) with analytical gradient procedures.[19,20] Their harmonic vibrational frequencies were calculated by diagonalizing the mass-weighted Cartesian force constant matrix, computed numerically by finite differences of analytical gradients.[28] From the UHF/3-21G calculated harmonic vibrational frequencies the zero-point vibrational energies were evaluated.

The interconversion between **1** and **2** was first studied by using the UHF version of the AM1 semiempirical SCF MO method,[29] employing a locally modified version[30] of the MOPAC program.[31] By starting at the equilibrium geometry of **1** and using the length of the breaking bond in **1** (C_2C_3) as the reaction coordinate, the energy being minimized with respect to all other geometrical

(14) Greig, G.; Thynne, J. C. C. *Trans. Faraday Soc.* **1966**, *62*, 3338.
(15) Greig, G.; Thynne, J. C. C. *Trans. Faraday Soc.* **1967**, *63*, 1369.
(16) Kerr, J. A.; Smith, A.; Trotman-Dickenson, A. F. *J. Chem. Soc. A* **1969**, 1400.
(17) Walsh, R. *Int. J. Chem. Kinet.* **1970**, *2*, 71.
(18) Boche, G.; Szeimies, G. *Angew. Chem., Int. Ed. Engl.* **1971**, *10*, 911.
(19) Schlegel, H. B. *J. Comput. Chem.* **1982**, *3*, 214.
(20) Murtagh, B. A.; Sargent, R. W. H. *Comput. J.* **1970**, *13*. 185.
(21) McIver, J. W.; Komornicki, A. *Chem. Phys. Lett.* **1971**, *10*, 303.
(22) Fukutome, H. *Prog. Theor. Phys.* **1972**, *47*, 1156.
(23) Jordan, K. D.; Silbey, R. *Chem. Phys. Lett.* **1973**, *18*, 27.
(24) Pople, J. A.; Nesbet, R. K. *J. Chem. Phys.* **1954**, *22*, 571.
(25) Binkley, J. S.; Pople, J. A.; Hehre, W. J. *J. Am. Chem. Soc.* **1980**, *102*, 939.
(26) Solē, A., unpublished. Most of the modifications made concern the implementation of the original VAX version of GAUSSIAN 80 on IBM computers running under the VM/CMS operating system.
(27) Binkley, J. S.; Whiteside, R. A.; Krishnan, R.; Seeger, R.; DeFrees, D. J.; Schlegel, H. B.; Topiol, S.; Kahn, L. R.; Pople, J. A. *QCPE* **1981**, *13*, 406.
(28) Pulay, P. *Mol. Phys.* **1969**, *17*, 197.
(29) Dewar, M. J. S.; Zoebisch, E. G.; Healy, E. F.; Stewart, J. J. P. *J. Am. Chem. Soc.* **1985**, *107*, 3902.
(30) Olivella, S., unpublished.
(31) Stewart, P. *QCPE Bull.* **1983**, *3*, 101. Olivella, S. *QCPE Bull.* **1984**, *4*, 109.

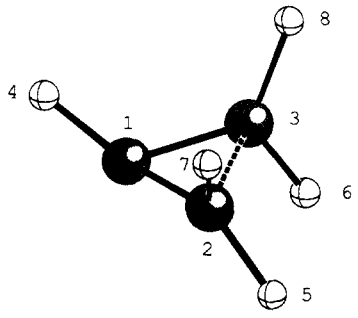

Figure 3. Computer plot of the optimized structure for the transition state interconverting cyclopropyl and allyl radicals.

variables without imposing any symmetry restrictions, a potential energy curve showing a continuous energy increase along the pathway leading to **2** was obtained. By use of the same reaction coordinate, another different potential energy curve was obtained starting at the equilibrium geometry of **2**, which showed again a continuous energy increase along the pathway leading to **1**. As might be expected for a symmetry-forbidden reaction, at the crossing point of both potential energy curves (the C_2C_3 bond length being ~2.0 Å) the structures corresponding to the first curve showed a cyclopropyl-like geometry (e.g., nearly C_s symmetry and no rotation of the methylene groups), while the structure corresponding to the second curve showed an allyl-like geometry (e.g., nearly C_{2v} symmetry with the methylene groups remaining in the plane of the carbon atoms). Subsequent geometry reoptimization of the cyclopropyl-like structure, *previously distorted to an nonsymmetric* (C_1) *geometry* (e.g., with unequal C_1C_2 and C_1C_3 bond lengths and one methylene group being rotated through 20° while the other remains orthogonal to the plane of the carbon atoms), by minimizing the norm of the scalar gradient,[32] led to a stationary point lying 24.5 kcal/mol above the AM1-calculated equilibrium geometry of **1**. This stationary point, was characterized as a transition structure by calculating and diagonalizing the force constant matrix (only one negative eigenvalue).

The AM1-calculated saddle point was taken as the initial geometry in a transition structure search using Schlegel's algorithm[19] with the UHF/3-21G wave function. The most relevant geometrical parameters of the resulting stationary point, hereafter referred to as TS, are given in Table I, where they are compared with the corresponding values obtained for the UHF/3-21G-optimized structures of **1** and **2**. Cartesian coordinates of all optimized structures of this investigation are available as supplementary material.

Geometrical Structure of the Transition State. The most salient features of TS are the unequal C_1C_2 and C_1C_3 bond lengths and the fact that the $C_2H_5H_7$ methylene group has rotated 16.9° (relative to its population in **1**) while the $C_3H_6H_8$ methylene group remains nearly orthogonal to the plane of the carbon atoms, the C_2C_3 bond length being stretched to 1.98 Å.

In order to characterize TS as a true transition structure, the harmonic vibrational frequencies were calculated at the UHF/3-21G level. The single imaginary frequency (789i cm^{-1}) corresponded primarily to the breaking of the C_2C_3 bond in **1** and the rotation of one methylene group ($C_2H_5H_7$). Interestingly, there was no indication of motion associated with the rotation of the other methylene group ($C_3H_6H_8$) in the transition vector. For the purpose of confirming that TS is the transition state that interconverts **1** and **2**, the intrinsic reaction coordinate (IRC) reaction path[34] connecting TS with both **1** and **2** was calculated, using a modified version[35] of the method of Ishida et al.,[36] as implemented in GAMESS system of programs.[37] By starting the IRC calculation at the saddle point TS and selecting as initial direction the transition vector with the sign that corresponds to the C_2C_3 bond forming, a smooth reaction path leading to **1** was obtained. Similarly, by selecting as initial direction the transition vector with the sign that corresponds to the C_2C_3 bond breaking, a reaction path was obtained leading to a structure with a geometry close to that of **2** but with one methylene group ($C_2H_5H_7$) nearly in the plane of the carbon atoms and the other remaining orthogonal to this plane. The latter indicates that the rotation of the second methylene group takes place in the last phase of the ring-opening process, namely, when the C_2C_3 bond is totally broken and the C_1C_2 π bond is fully formed. This nonsynchronous rotation of the two methylene groups in the ring opening of **1** implies that *the thermal conversion of* **1** *into* **2** *takes place via a transition state that is common to both the disrotatory and conrotatory modes of reaction.*

Table I. Selected Geometrical Parameters[a] of the UHF/3-21G-Optimized Structures for Cyclopropyl Radical (**1**), Allyl Radical (**2**), and the Transition State (TS) for the Thermal Interconversion between **1** and **2**

	1	TS	**2**
molec sym	C_s	C_1	C_{2v}
	Bond Lengths, Å		
C_1C_2	1.486	1.436	1.389
C_1C_3	1.486	1.484	1.389
C_2C_3	1.534	1.980	2.455
	Bond Angles, deg		
$C_2C_1C_3$	62.1	85.4	124.3
$H_5C_2H_7$	114.9	117.4	117.5
$H_6C_3H_8$	114.9	119.4	117.5
	Bond–Plane Angles, deg		
$(H_4C_1)(C_1C_2C_3)$	139.1	139.9	180.0
$(C_1C_2)(H_5C_2H_7)$	151.9	173.4	180.0
$(C_1C_3)(H_6C_3H_8)$	151.9	175.3	180.0
	Plane–Plane Angles, deg		
$(C_1C_2C_3)(H_5C_2H_7)$	89.7	72.8	0.0
$(C_1C_2C_3)(H_6C_3H_8)$	89.7	86.9	0.0

[a] Atom numbering as in Figure 3.

Relative Energies. The total and relative energies, along with the zero-point vibrational energies, of **1**, TS, and **2**, calculated at the UHF/3-21G level of theory, are given in Table II. The potential energy barrier for the formation of **2** from **1** via TS is 22.4 kcal/mol at the UHF/3-21G level and becomes 19.2 kcal/mol after including the zero-point vibrational energy correction. The latter value is in good agreement with the approximate experimental activation energies, ranging from 19.1 to 22 kcal/mol. However, this agreement may be fortuitous since our theoretical model is subject to considerable error because it does not explicitly include electron correlation and the basis set used is relatively small. In this connnection it is instructive to examine the expectation values of the spin-squared operator S^2, $\langle S^2 \rangle$, for the UHF/3-21G wave function of **1** and TS, which are listed in Table III. While for **1** the value (0.762) of $\langle S^2 \rangle$ is close to the expected value (0.75) for a pure doublet wave function, the value (1.149) for TS differs significantly from this ideal value. The latter indicates considerable spin contamination from states of higher multiplicity (i.e.; quartet, sextet, etc.) in the UHF/3-21G wave function of TS. However, annihilation of the next highest spin contaminant in this wave function leads to $\langle S^2 \rangle = 0.765$. This shows that the main spin contaminant state in the UHF wave function of TS is the first quartet state. According to UHF theory, it is the $\langle S_z \rangle = +^1/_2$ component of this quartet state that mixes into the UHF doublet wave function. In the single-configuration approach, the wave function of the $\langle S_z \rangle = +^1/_2$ component of the first quartet state can be written in short form as[38]

$$^4\Phi = (3)^{-1/2}\{|...\phi_i\phi_k\bar{\phi}_m| + |...\phi_i\bar{\phi}_k\phi_m| + |...\bar{\phi}_i\phi_k\phi_m|\} \quad (7)$$

(32) By using the NLLSQ procedure.[33]
(33) Bartels, R.; Weiner, P. K., unpublished.
(34) Truhlar, D. G.; Kuppermann, A. *J. Am. Chem. Soc.* **1971**, *93*, 1840. Fukui, K. *Acc. Chem. Res.* **1981**, *14*, 363.
(35) Schmidt, M. W.; Gordon, M. S.; Dupuis, M. *J. Am. Chem. Soc.* **1985**, *107*, 2585.
(36) Ishida, K.; Morokuma, K.; Komornicki, A. *J. Chem. Phys.* **1977**, *66*, 2153.
(37) Dupuis, M.; Spangler, D.; Wendoloski, J. J. *Natl. Resour. Comput. Chem. Software Cat.* **1980**, *1*, QG01. Extended by M. W. Schmidt and S. T. elbert, 1988.
(38) Longuet-Higgins, H. C.; Pople, J. A. *Proc. Phys. Soc.* **1955**, *A68*, 591.

Table II. Calculated Total Energies (Hartrees) and Zero-Point Vibrational Energies (kcal/mol) for Cyclopropyl Radical (1), Allyl Radical (2), and the Transition State (TS) for the Thermal Interconversion between 1 and 2[a,b]

species	state	UHF/3-21G	ROHF/3-21G	UHF/6-31G*	ZPE
1	$^2A'$	-115.75662 (0.0)	-115.75426 (0.0)	-116.41501 (0.0)	45.2
TS	^2A	-115.72100 (22.4)	-115.70677 (29.8)	-116.36291 (32.7)	42.0
2	$^2A_2$	-115.82304 (-41.7)	-115.79702 (-26.8)	-116.46808 (-33.3)	43.8

[a] All calculations at the UHF/3-21G-optimized geometries. [b] The quantities in parentheses are the relative energies in kilocalories per mole.

Table III. Expectation Values of S^2 for the UHF Wave Function of Cyclopropyl Radical (1), Allyl Radical (2), and the Transition State (TS) for the Thermal Interconversion between 1 and 2[a]

		UHF/3-21G		UHF/6-31G*	
species	state	BA[b]	AA[c]	BA[b]	AA[c]
1	$^2A'$	0.762	0.750	0.761	0.750
TS	^2A	1.149	0.765	1.088	0.762
2	$^2A_2$	0.975	0.759	0.971	0.758

[a] All calculations at the UHF/3-21G-optimized geometries. [b] Before annihilation of the quartet-state component. [c] After annihilation of the quartet-state component.

Table IV. Occupation Numbers of the Relevant Natural Orbitals of the UHF/3-21G Wave Function of Cyclopropyl Radical (1), Allyl Radical (2), and the Transition State (TS) for the Thermal Interconversion between 1 and 2

species	state	natural orbitals		
1	$^2A'$	7a'	8a'	5a''
		1.9972	1.0000	0.0028
TS	^2A	11a	12a	13a
		1.7849	1.0000	0.2151
2	$^2A_2$	$1b_1$	$1a_2$	$2b_1$
		1.8933	1.0000	0.1067

where ϕ_i, ϕ_m, and ϕ_k represent the highest doubly occupied, the singly occupied, and the lowest unoccupied MOs of TS. At this point we note that the admixture of the above quartet state with the ground-state doublet occurring in the UHF wave function of TS allows for some electron correlation effect between orbitals of different spin, resulting in an energy lowering of TS relative to 1. In order to evaluate from an energetic point of view the importance of this electron correlation effect, additional single-point spin-restricted open-shell Hartree–Fock (ROHF)[39] calculations with the 3-21G basis set were performed at the UHF/3-21G-optimized geometries of 1, TS, and 2, using the GAMESS system of programs. The total and relative energies calculated at this level of theory (denoted ROHF/3-21G) are given in Table II. It turns out that whereas for 1 the ROHF/3-21G energy is 1.5 kcal/mol higher than when calculated at the UHF/3-21 level, for TS the ROHF/3-21G energy is 8.9 kcal/mol higher than when calculated with the UHF/3-21G wave function. Therefore, it follows that the energy lowering due to the electron correlation implicitly included in the UHF/3-21G wave function, because of the aforementioned mixing of the quartet and doublet states, is 7.4 kcal/mol larger for TS, as compared to 1.

The energy of reaction for the isomerization of 1 to 2, calculated at the UHF/3-21G level (-41.7 kcal/mol), is about twice the enthalpy of reaction, -22.8 ± 4.9 kcal/mol, estimated from the observed[40] heats of formation of 2 and 1 (i.e., 43.7 ± 2.2 and 66.5 ± 2.7 kcal/mol, respectively). It is well-known that the 3-21G basis set gives a balanced description of the relative energies of the σ and π bonds, but since the polarization functions are not included, ring strain is overestimated.[41] This tends to lower the energy of 2 relative to that of 1. In order to corroborate this point, additional single-point UHF calculations were carried out with the larger split-valence plus d polarization at the carbon atoms 6-31G* basis set.[42] The total and relative energies calculated at the UHF/6-31G* level are included in Table II and $\langle S^2 \rangle$ values of the corresponding wave functions are listed in Table II. The energy of reaction for the isomerization of 1 or 2 at this level of theory is calculated to be -33.3 kcal/mol. Therefore, though the addition of polarization functions to the basis set improves substantially the calculated energy difference between 1 and 2, the UHF model appears to underestimate the energy of 2 with respect to that of 1. In this connection, it is instructive again to examine the values of $\langle S^2 \rangle$ for the UHF wave function of 1 and 2. Considering for example the 3-21G basis set, inspection of Table III reveals that whereas for 1 the value (0.762) of $\langle S^2 \rangle$ points out that the contamination by higher spin states is unimportant, the value (0.975) for 2 indicates significant mixing of the first quartet state into the UHF/3-21G doublet wave function. The latter is due to the so-called "spin or exchange polarization" phenomenon, which arises from the unusual exchange interaction between the odd electron and the two bonding π electrons in 2.[43] Roughly speaking, the odd electron (described by the $1a_2$ MO, which is completely localized on the end carbon atoms of 2) "attracts" the bonding π electron of the same spin (described by a b_1 MO) toward the end carbon atoms, while the bonding π electron of opposite spin (described by a slightly different b_1 MO) is more concentrated in the central carbon atom. The essential result is that in 2 the UHF model introduces some additional electron correlation effect between the two bonding π electrons that is not included in 1, and consequently, at this level of theory the energy of 2 is artificially lowered relative to that of 1. By comparing the UHF/3-21G and ROHF/3-21G energies shown in Table II, the energy lowering of 2 with respect to 1, introduced by the UHF model, is evaluated to be 14.9 kcal/mol. With this correction, the UHF/6-31G* calculated energy of the reaction (-33.3 kcal/mol) for the isomerization of 1 to 2 becomes -18.4 kcal/mol. After including the zero-point vibrational energy correction to the latter value, the resulting energy of reaction (-19.8 kcal/mol) is brought into satisfactory agreement with the experimental enthalpy of reaction (-22.8 ± 4.9 kcal/mol).

Multiconfiguration SCF Calculations

According to the present consensus, the calculation of transition structures requires a multiconfiguration (MC) SCF wave function for appropriate description of the zeroth-order electron correlation (i.e., the nondynamical or strong correlation).[44] In this approach the most frequently used MCSCF wave function involves a complete CI in a limited set of valence orbitals, the "active space". This complete active space (CAS)[45] [also called fully optimized reaction space (FORS)[46]] MCSCF method, designated CASSCF, has become widely popular because it simplifies the problem of selecting the length and type of the MCSCF expansion.

In order to assess the reliability of the interesting results obtained in the previous section, i.e., the existence of a common nonsymmetric transition state for both the conrotatory and disrotatory thermal interconversion between 1 and 2, we undertook

(39) Roothaan, C. C. J. *Rev. Mod. Phys.* **1960**, *32*, 179. Davidson, E. R. *Chem. Phys. Lett.* **1973**, *21*, 565.
(40) DeFrees, D. J.; McIver, R. T.; Hehre, W. J. *J. Am. Chem. Soc.* **1980**, *102*, 3334.
(41) Hehre, W. J.; Radom, L.; Schleyer, P. v. R.; Pople, J. A. *Ab Initio Molecular Orbital Theory*; John Wiley: New York, 1986; pp 290–298.
(42) Hariharan, P. C.; Pople, J. A. *Theor. Chim. Acta* **1973**, *28*, 213.
(43) See, for example: Salem, L. *The Molecular Orbital Theory of Conjugated Systems*; Benjamin: New York, 1966; pp 72–74.
(44) Sinanoglu, O.; Brueckner, K. A. *Three Approaches to Electron Correlation in Molecules*; Yale University: New Haven, CT, 1970.
(45) Roos, B. O.; Taylor, P. R.; Siegbahn, P. E. M. *Chem. Phys.* **1980**, *48*, 157. Roos, B. O. *Adv. Chem. Phys.* **1987**, *69*, 399.
(46) Ruedenberg, K.; Sundberg, K. R. *Quantum Science*; Calais, J. L., Gocinski, O., Linderberg, J., Ohrn, Y., Eds.; Plenum Press: New York, 1976; pp 505–515. Cheung, L. M.; Sundberg, K. R.; Ruedenberg, K. *Int. J. Quantum Chem.* **1979**, *16*, 1103. Ruedenberg, K.; Schmidt, M. W.; Gilbert, M. M.; Elbert, S. T. *Chem. Phys.* **1982**, *71*, 41, 51, 65.

a reinvestigation of the ring opening of **1** into **2** by using a CASSCF treatment.

Computational Details. In the present work, the determination of the complete active space was performed by the procedure recently suggested by Pulay and Hamilton.[47] These authors have shown that the natural orbitals of the UHF wave function, designated UNOs, provide an automatic CAS selecting procedure and excellent starting orbitals for CASSCF calculations in regions of the potential energy surface where the electron correlation is nondynamical. The active space should include the UNOs with significant fractional occupation, say between 0.02 and 1.98. UNOs with occupancy above 1.98 are doubly occupied, and those with occupancy below 0.02 are left empty.

Table IV lists the occupation numbers of the relevant UNOs of **1**, TS, and **2**, determined from the UHF/3-21G wave function. In the case of TS and **2**, the fractional occupancies of the UNOs indicate that there are three "active" orbitals, hereafter denoted ϕ_i, ϕ_m, and ϕ_k, where ϕ_m is the MO describing the unpaired electron. As might be expected for TS, ϕ_i and ϕ_k are the bonding and antibonding MOs of the CC bond being broken (i.e., C_2C_3), respectively. As regards to **2**, ϕ_i and ϕ_k are the highest doubly occupied and the lowest unoccupied π MOs, respectively. In passing, we may note that the fractional occupancy shown by the $1b_1$ and $2b_1$ UNOs of **2** is clearly related to the aforementioned "spin or exchange polarization" phenomenon shown by the UHF wave function of this radical. In the case of **1**, it turns out that there is not any significant fractional occupancy of the UNOs (see Table IV). This indicates that in the region of the potential surface around the equilibrium geometry of **1** the electron correlation is dynamical; consequently there are no "active" orbitals, beside the MO describing the unpaired electron. Nevertheless, for reasons of continuity, it is desirable to extend the MCSCF calculations to such a region of the potential surface, the MCSCF expansion and the nature of the orbitals being defined by analytical continuation from the neighboring strongly correlated region around the geometry of TS. Thus, for **1** the bonding (σ_{CC}) and antibonding (σ_{CC}*) MOS of the CC bond to be broken were taken as the "active" orbitals ϕ_i and ϕ_k, respectively, and the 8a′ MO as the "active" orbital ϕ_m. The starting ϕ_i was easily chosen after localizing (by using Boys' method[48]) the set of the occupied α-spin UHF/3-21G MOs of **1**. The starting ϕ_k was selected from the set of the virtual α-spin UHF/3-21G MOs on the basis of the required nodal (i.e., C_2C_3 antibonding) properties. Distribution of the three reacting electrons within the three "active" orbitals with all possible couplings leads to a MCSCF wave function formed as a linear combination of eight doublet spin-adapted configuration state functions (CSFs).

All CASSCF calculations were carried out by using the GAMESS system of programs, which includes the Newton–Raphson orbital procedure for MCSCF wave functions.[49] Starting with the UHF/3-21G-optimized structures, the equilibrium geometries of **1** and **2**, as well as the geometry of the transition state TS, were completely reoptimized by using the 3-2G basis set with analytical gradient procedures.[19,20] Their harmonic vibrational frequencies were calculated with the same basis set by diagonalizing the mass-weighted Cartesian force constant matrix, computed numerically by finite differences of analytical gradients. From the harmonic vibrational frequencies the zero-point vibrational energies were evaluated.

Geometrical Structures. The relevant geometrical parameters of the structures optimized with the CASSCF/3-21G wave function are given in Table V. The equilibrium geometries of **1** and **2** do not differ appreciably from those calculated with the UHF/3-21G wave function (Table I), the most salient difference being in the C_2C_3 bond length, which is found to be 0.041 Å longer at the CASSCF/3-21G level. This result is consistent with the fact that the latter wave function includes explicitly the correlation between the two electrons forming the C_2C_3 bond. As regards the equilibrium geometry of **2**, we note that it has previously been reported by Takada and Dupuis[50] in a MCSCF/3-21G study of the structure and vibrational analysis of this radical.

Table V. Selected Geometrical Parameters[a] of the CASSCF/3-21G-Optimized Structures for Cyclopropyl Radical (**1**), Allyl Radical (**2**), and the Transition State (TS) for the Thermal Interconversion between **1** and **2**

	1	TS	**2**
molec sym	C_s	C_1	C_{2v}
	Bond Lengths, Å		
C_1C_2	1.485	1.424	1.388
C_1C_3	1.485	1.485	1.388
C_2C_3	1.575	2.066	2.455
	Bond Angles, deg		
$C_2C_1C_3$	64.1	90.5	124.3
$H_5C_2H_7$	115.4	117.3	117.4
$H_6C_3H_8$	115.4	119.2	117.4
	Bond–Plane Angles, deg		
$(H_4C_1)(C_1C_2C_3)$	138.6	138.9	180.0
$(C_1C_2)(H_5C_2H_7)$	153.2	175.8	180.0
$(C_1C_3)(H_6C_3H_8)$	153.2	175.3	180.0
	Plane–Plane Angles, deg		
$(C_1C_2C_3)(H_5C_2H_7)$	89.7	66.0	0.0
$(C_1C_2C_3)(H_6C_3H_8)$	89.7	86.1	0.0

[a] Atom numbering as in Figure 3.

In comparing Tables I and V, it is readily seen that the CASSCF and UHF wave functions with the 3-21G basis set give similar optimized geometries for the transition state of the thermal interconversion between **1** and **2**. The main structural differences are the C_2C_3 bond length and the angle between the plane of the $C_2H_5H_7$ methylene group and the plane of the carbon atoms, which are predicted to be 0.086 Å longer and 6.8° smaller, respectively, by the CASSCF wave function. The single imaginary frequency (1149i cm^{-1}), determined by using the latter wave function, again corresponded primarily to the breaking of the C_2C_3 bond in **1** and the rotation of one methylene group ($C_2H_5H_7$). Furthermore, there was no indication of motion associated with the rotation of the other methylene group ($C_3H_6H_8$) in the transition vector. These results confirm the conclusions drawn from the previous UHF study of the thermal ring opening of **1** and **2**, in the sense that on the ground-state potential energy surface there is a single nonsymmetric transition structure interconverting these minima, so both the conrotatory and disrotatory modes have a common transition state.

Relative Energies. The total and relative energies, along with the zero-point vibrational energies, of **1**, TS, and **2**, calculated by using the CASSCF/3-21G wave function, are given in Table VI. The predicted potential energy barrier for the formation of **2** from **1** via TS is 19.6 kcal/mol at the CASSCF/3-21G level and becomes 16.6 kcal/mol after including the zero-point vibrational energy correction. The latter value is 2.5 kcal/mol smaller than the lower limit of the approximate experimental activation energies, ranging from 19.1 to 22 kcal/mol.

From the theoretical point of view, it is interesting to note that the activation barrier calculated at the CASSCF/3-21G level differs only in 2.8 kcal/mol from that determined at the UHF/3-21G level (see Table II). In this connection, it is worthwhile to examine the CI coefficients of the MCSCF expansions of **1**, TS, and **3**. These are listed in Table VII for the electron configurations contributing 1% or more to the CASSCF/3-21G wave function. First of all, we note that in each case, besides the ground-state electron configuration, which always has the largest contribution, there are one singly and one doubly excited configurations (relative to the ground-state configuration) contributing significantly to the MCSCF expansion. The doubly excited configuration is one in which two electrons are raised from ϕ_i to ϕ_k. By mixing this doubly excited configuration with the

(47) Pulay, P.; Hamilton, T. P. *J. Chem. Phys.* **1988**, *88*, 4926.
(48) Boys, S. F. *Rev. Mod. Phys.* **1960**, *32*, 296.
(49) Yaffe, L. G.; Goddard, W. A. *Phys. Rev. A* **1976**, *13*, 1682.
(50) Takada, T.; Dupuis, M. *J. Am. Chem. Soc.* **1983**, *105*, 1713.

Table VI. Calculated Total Energies (Hartrees) and Zero-Point Vibrational Energies (kcal/mol) for Cyclopropyl Radical (**1**), Allyl Radical (**2**), and the Transition State (TS) for the Thermal Interconversion between **1** and **2**[a,b]

species	state	CASSCF/3-21G	TCSCF/3-21G	CASSCF/6-31G*	ZPE
1	$^2A'$	-115.77189 (0.0)	-115.77159 (0.0)	-116.42876 (0.0)	44.9
TS	^2A	-115.74070 (19.6)	-115.72957 (26.4)	-116.38913 (24.9)	41.9
2	$^2A_2$	-115.84024 (-42.9)	-115.80899 (-23.5)	-116.48356 (-34.3)	43.7

[a] All calculations at the CASSCF/3-21G-optimized geometries. [b] The quantities in parentheses are the rellative energies in kilocalories per mole.

Table VII. List of Configurations Contributing 1% or More to the CASSCF Wave Functions of Cyclopropyl Radical (**1**), Allyl Radical (**2**), and the Transition State (TS) for the Thermal Interconversion between **1** and **2**

		CI mixing coefficients		electronic configuration		
species	state	3-21G	6-31G*			
1	$^2A'$			7a′	8a′	5a″
		-0.929	-0.931	2	1	0
		-0.351	-0.347	1	2	0
		0.105	0.103	0	1	2
TS	^2A			11a	12a	13a
		-0.931	-0.936	2	1	0
		0.252	0.244	0	1	2
		0.249	0.238	1	1	1
2	$^2A_2$			$1b_1$	$1a_2$	$2b_1$
		-0.958	-0.960	2	1	0
		-0.245	-0.241	1	1	1
		0.147	0.144	0	1	2

ground-state configuration, the MCSCF wave function correlates either the two electrons forming the C_2C_3 bond in **1** and TS or the two bonding π electrons in **2**. As regards the singly excited configurations, in the case of **1** it is one in which an electron is raised from ϕ_i to ϕ_m. This is the only singly excited configuration that has the appropriate symmetry (A′) to interact with the ground-state configuration of **1**. In sharp contrast, the singly excited configuration contributing 1% or more to the CASSCF/3-21G of TS and **2** is one of the two doublet spin-adapted CSFs associated with the excited configuration generated by promotion of one electron from ϕ_i to ϕ_k. Specifically, this CSF can be written in short form as[38]

$$^2\Phi = (6)^{-1/2}\{2|...\phi_i\phi_k\bar{\phi}_m| - |...\phi_i\bar{\phi}_k\phi_m| - |...\bar{\phi}_i\phi_k\phi_m|\} \quad (8)$$

At this point we note that the spatial function of eq 8 is closely related to that of the CSF assigned to the $\langle S_z\rangle = +^1/_2$ component of the quartet state that mixes into the UHF doublet wave function of TS and **2**, given by eq 7. It is also worthy of mention that Kikuchi has shown that the inclusion of this CSF in the MCSCF expansion is sufficient to obtain the correct C_{2v} structure of this radical.[51]

In order to evaluate approximately the contribution of the above singly excited configurations to the correlation energy of **1**, TS, and **2**, single-point two-configuration (TC) SCF calculations were carried out with the 3-21G basis set at the CASSCF/3-21G-computed geometries. In addition to the ground-state doublet configuration, this TCSCF wave function included the aforementioned doubly excited configuration, namely $(\phi_i)^2 \rightarrow (\phi_k)^2$. The total energies calculated with such TCSCF wave function are given in Table VI. In comparing the total energies calculated at the CASSCF and TCSCF levels of theory, it is noteworthy that the addition of the relevant singly excited configurations (given in Table VII) to the TCSCF expansion of **1** and TS leads to an energy lowering of 0.2 and ~6.9 kcal/mol, respectively. Therefore, it turns out that the inclusion of the CSF given by eq 8 in the wave function of TS lowers the activation barrier for the conversion of **1** into **2** by ~7 kcal/mol. It may be noted that such an energy lowering of TS is nearly identical with the relative stabilization energy (7.4 kcal/mol) determined above in the UHF/3-21G treatment of this species, which arises from the admixture of the quartet configuration (i.e., the CSF given by eq 7) into the UHF doublet wave function. The latter result accounts in part for the aforementioned agreement between the activation barriers calculated with the 3-21G basis set at the UHF and CASSCF levels of theory.

It is interesting to note that all attempts to locate a transition structure interconverting **1** and **2** by using the above TCSCF/3-21G wave function were unsuccessful. It turns out, therefore, that in order to describe adequately such a transition structure, the MCSCF expansion must include the CSF given by eq 8. Apparently, besides the aforementioned doubly excited configuration, which is required to mix with the ground-state configuration in order to correlate the electron pair of the bond undergoing rupture, the spin coupling in the CSF given by eq 8 is essential to describe the electronic changes that take place at the transition state. These consist in starting the formation of a CC π bond by coupling the formerly unpaired electron in **1** with one of the two electrons of the CC bond being broken while the other electron is localized on the carbon atom of the methylene group, which remains orthogonal to the plane of the carbon atoms. In the case of the UHF treatment, the spin coupling in the $\langle S_z\rangle = +^1/_2$ component of the quartet state that mixes into the doublet UHF wave function (given by eq 7) plays the role of the relevant singly excited configuration (given by eq 8) included in the CASSCF expansion.

At the CASSCF/3-21G level, the energy of reaction (-42.9 kcal/mol) calculated for the rearrangement of **1** to **2** is 1.2 kcal/mol lower than that (-41.7 kcal/mol) determined by using the UHF/3-21G wave function. Moreover, from the CASSCF/3-21G total energy of **1** and the TCSCF/3-21G energy of **2** (see Table VI), it follows that the exclusion of the CSF given by eq 8 from the CASSCF/3-21G wave function of TS leads to an energy of reaction of -23.7 kcal/mol, which is only -3.1 kcal/mol higher than the value obtained from the ROHF/3-21G. These results suggest that there is a parallelism between the overstabilization of **2** relative to **1** found in the UHF treatment, due to the mixing of the first quadruplet state into the doublet wave function of **2**, and the overstabilization of **2** relative to **1** found in the CASSCF formalism, due to the inclusion of the CSF given by eq 8 in the MCSCF expansion of **2**.

In order to test the effect of the d polarization functions (at the carbon atoms) on the relative energies of **1**, TS, and **2**, single-point CASSCF calculations were performed with the 6-31G* basis set at the CASSCF/3-21G-optimized geometries. The resulting total and relative energies are given in Table VI, and the CI coefficients of the configurations contributing 1% or more to the CASSCF/31G* wave function are listed in Table VII. In comparing Tables II and VI, it is readily seen that the inclusion of polarization functions decreases the energy difference between **1** and **2** by about the same value (~8.5 kcal/mol) in both the UHF and CASSCF treatments. Furthermore, it turns out that, as noted in the case of the UHF/6-31G* treatment, the CASSCF/6-31G* model underestimates the energy of **2** with respect to that of **1**. Again, this result suggests that the change in electron correlation energy associated with the isomerization of **1** to **2** is not adequately described by the CASSCF wave function. Better agreement between the calculated energy of reaction and the experimental heat of isomerization can only be obtained by including dynamical electron correlation effects, for example, by means of either multireference (MR) CI[52] or many-body perturbation theory[53] calculations, based on the

(51) Kikuchi, O. *Chem. Phys. Lett.* **1980**, *72*, 487.

(52) For a review, see: Shavitt, I. In *Modern Theoretical Chemistry*; Schaefer, H. F., III, Ed.; Plenum Press: New York, 1977; Vol. 3.

(53) For a review, see: Barlett, R. J. *Annu. Rev. Phys. Chem.* **1981**, *32*, 359.

CASSCF/6-31G* wave functions of **1** and **2** as the zeroth-order wave functions. Such correlated calculations are beyond the scope of the present investigation.

Regarding the activation barrier for the conversion of **1** into **2**, it should be noted that the value calculated at the CASSCF/6-31G* level is 5.3 kcal/mol higher than the calculated at the CASSCF/3-21G level. This result is consistent with the aforementioned fact that the 3-21G basis set overestimates the ring strain in **1**. Finally, at the highest level of theory employed in this investigation, namely, from the CASSCF/6-31G*//CASSCF/3-21G-calculated energies and the zero-point energy correction obtained from the CASSCF/3-21G-calculated vibrational frequencies, the activation barrier for the ring opening of **1** into **2** is predicted to be 21.9 kcal/mol, in excellent agreement with the experimental activation energies ranging from 19.1 to 22 kcal/mol.

Conclusions

The following conclusions can be drawn from the ab initio UHF and CASSCF calculations reported here: (1) In qualitative agreement with early MINDO/3 calculations by Dewar and Kirschner, the thermal ring opening of **1** to give **2** takes place via a highly nonsymmetric transition state whose geometry shows unequal C_1C_2 and C_1C_3 bond lengths, with one methylene group having rotated $\sim 24°$ (relative to its position in **1**) whereas the other remains nearly orthogonal to the plane of the carbon atoms, the length of the CC undergoing rupture being ~ 2 Å.

(2) According to both the transition vector of this transition state and the IRC reaction path, the rotation of the second methylene group takes place in the last phase of the ring-opening process, namely, when the C_2C_3 bond is totally broken and the C_1C_2 π bond is fully formed. This nonsynchronous rotation of the two methylene groups implies that the thermal conversion of **1** into **2** involves a common transition state for both the conrotatory and disrotatory modes of reaction. Therefore, in the absence of substituents in the methylene groups, which may lead to steric effects, there should be no special preference between the conrotatory and disrotatory modes. An experimental test of this interesting prediction is obviously highly desirable.

(3) In order to locate a transition structure for the ring opening of **1** into **2** it is necessary to use a MCSCF wave function whose CI expansion includes the singly excited configuration in which one electron is raised from the highest doubly occupied MO to the lowest unoccupied MO. This configuration appears to be essential to describe the electronic changes that take place at the transition state.

(4) Due to the substantial mixing of the $\langle S_z \rangle = +^1/_2$ component of the first quartet state into the UHF/3-21G doublet wave function, the latter method enables the calculation of a transition state for the ring opening of **1** into **2** whose geometry is similar to that found by using the CASSCF/3-21G model. Furthermore, the activation barrier calculated at the UHF/3-21G level differs only in 2.8 kcal/mol from that determined at the CASSCF/3-21G level. Therefore, the UHF/3-21G model is a good starting point to locate transition structures for the ring-opening reactions of cycloalkyl radicals.

Acknowledgment. This work was supported by the CICYT (Grant PB86-0270). The calculations were carried out with the IBM 4381 computer at the Centre d'Informàtica de la Universitat de Barcelona. We are indebted to Dr. Michael W. Schmidt (North Dakota State University) for providing us a copy of his greatly extended version of the GAMESS system of programs.

Registry No. 1, 2417-82-5; **2**, 1981-80-2.

Supplementary Material Available: Listing of Cartesian coordinates of the optimized molecular structures of **1**, TS, and **2**, calculated at the UHF/3-21G and CASSCF/3-21G levels of theory (3 pages). Ordering information is given on any current masthead page.

Sustained Oscillations and Bistability in a Detailed Mechanism of the Peroxidase–Oxidase Reaction

Baltazar D. Aguda and Raima Larter*

Contribution from the Department of Chemistry, Indiana University-Purdue University at Indianapolis, Indianapolis, Indiana 46205. *Received August 4, 1989*

Abstract: A detailed mechanism for the aerobic oxidation of NADH catalyzed by horseradish peroxidase, called the peroxidase–oxidase reaction, is studied by computer simulation and found to show bistability, damped and sustained oscillations. These oscillations are smooth and almost sinusoidal. The mechanism also predicts that a stable oscillatory state and a stable steady state can coexist for the same set of parameters. Decreasing the oxygen concentration in the gas phase for a short period of time is found to perturb the stable steady state toward the oscillatory state, while a spike of hydrogen peroxide drives an oscillatory state to a stable steady state. The mechanism is compared with detailed mechanisms proposed by other investigators as well as two 4-species abstract models we have studied previously.

I. Introduction

Enzymes called peroxidases catalyze the oxidation of a large variety of organic substances using hydrogen peroxide. Because molecular oxygen can undergo a series of free radical reactions leading to hydrogen peroxide, some peroxidases can also catalyze the oxidation of a small number of hydrogen donors by oxygen. These hydrogen donors include nicotinamide adenine dinucleotide (NADH), nicotinamide adenine dinucleotide phosphate (NADPH), dihydroxyfumaric acid, indoleacetic acid, and triose reductone.[1] In this paper, we will only consider the peroxidase enzyme-catalyzed aerobic oxidation of NADH and refer to it as the peroxidase–oxidase (PO) reaction.[2] The stoichiometry of the overall reaction is

$$2NADH + O_2 + 2H^+ \rightarrow 2NAD^+ + 2H_2O \qquad (1)$$

When this reaction is carried out in an open system in which oxygen is continuously supplied to a well-stirred solution of NADH

(1) Olsen, L.; Degn, H. *Biochim. Biophys. Acta* **1978**, *523*, 321.
(2) Degn, H.; Olsen, L.; Perram, J. *Ann. N.Y. Acad. Sci.* **1979**, *316*, 623.

0002-7863/90/1512-2167$02.50/0